

ZONAL FLOWS BELOW THE SUN'S CONVECTION: ANALYTIC APPROXIMATION

by

Charles L. Wolff & Hans G. Mayr

POPULAR SUMMARY

We have derived a simple analytic solution showing how the Sun's global oscillations (g-modes) can drive east-west flows at low latitude deep inside the Sun. This flow is analogous to the Quasi Biennial Oscillation in the Earth's upper atmosphere. It has an observed period of 1.3 years in the solar case but its cause was not known until we published an explanation in a Letter to the Editor a few months ago. Now we give full details of the model and show how it can be used to limit the range of g-modes that can be actively driving the reversing flows. A nonlinear feedback feature of the model is that the flow itself creates the turbulent dissipation that extracts momentum from the g-modes that, in turn, drives the flow.

ZONAL FLOWS BELOW THE SUN'S CONVECTION: ANALYTIC APPROXIMATION

CHARLES L. WOLFF and HANS G. MAYR
NASA Goddard Space Flight Center, Greenbelt, MD 20771
charles.wolff@nasa.gov, hans.g.mayr@nasa.gov

ABSTRACT

The low latitude zonal flows detected beneath the Sun's convective envelope (CE) are modelled as a wave with 1.3 yr period running toward the solar center with exponentially diminishing amplitude. The flows have sufficient shear in latitude to make them horizontally unstable, creating a large diffusivity $\sim 10^9$ to $10^{10} \text{ m}^2\text{s}^{-1}$. As this turbulence locally dissipates g-modes, they deposit zonal momentum that sustains the flow. "Wave filtering" causes some of the momentum to be deposited in proper phase to advance the flow downward, analogous to flows seen in the Earth's upper atmosphere. The analytic model shows the effect of a "typical pair" of g-modes (angular harmonic ℓ and oscillation frequency σ_0) acting alone to drive the flow. Their efficiency in driving a flow is proportional to at least m^3 , the zonal harmonic number. Thus high harmonic modes with $|m| \cong \ell$ are of most interest and are used in numerical examples. Taking the free parameters to be ℓ and σ_0 , the analytic model yields just one peak flow velocity V_0 and one g-mode amplitude that is acceptable for each choice, (ℓ, σ_0) . After future measurements constrain V_0 to a small part of its currently uncertain range (5 to perhaps 100 m/s) there will be only one free parameter instead of two, and our model will provide a relation $\sigma_0(\ell)$ that constrains those g-modes that can be mainly responsible for driving the flow.

Subject headings: Fluid Dynamics—Sun: oscillations—Sun: interior

1. INTRODUCTION

East-west flows that reverse direction about every 1.3 yr are observed in the Sun (Howe, *et al.* 2000; Antia & Basu 2000; Komm, *et al.* 2003) below the convective envelope (CE) at low latitudes. Analogous flows in the Earth's upper atmosphere are driven by gravity waves (Dunkerton 1997; Mayr, *et al.* 1997, 2000) and since the Sun's CE excites such waves, initial explanations of the solar flow were based on a flux of gravity waves propagating downward from the CE (Fritts, Vadas, & Andreassen 1998; Kim & MacGregor 2001, 2003; Talon, Kumar, & Zahn 2002). A rich progression of theoretical flows (steady, periodic, quasi-periodic, chaotic) was demonstrated by Kim & MacGregor (2001) as the ratio of viscosity to gravity wave strength was decreased. These gravity wave models, however, apply only to a thin

layer ($< 0.02R_\odot$) immediately below the CE and do not explain the bulk of the observed 1.3 yr flows (Wolff & Mayr 2004, hereafter Paper I). This is true because gravity wave models depend on vertical turbulence, which does not extend below that thin layer (Schatzman, Zahn & Morel 2000).

A new approach was suggested in Paper I invoking global oscillations (g-modes) excited in the Sun's core and partially dissipated by horizontal turbulence below the CE. As the flow generates this turbulence, energy and momentum flux is extracted from the g-modes to accelerate the flow. Eventually the turbulence grows to limit the maximum flow speed. In the present paper, we describe this model more fully and present a simplified analytic solution suitable for estimating the parameter range for the reversing flow and the g-modes that generate it. Only two properties of a g-mode are used: its spherical harmonic amplitude distri-

bution and its dispersion relation in the limit that the square of the oscillation frequency, $\sigma^2 \ll \bar{N}^2$. (Here \bar{N} is the buoyancy frequency typical of the shell, 0.6 to 0.7 R_\odot , containing most of the flow energy.) The CE is not considered since g-mode amplitudes there decline rapidly with height, and the flow energy would be comparatively small.

After an overall description in §2, we give in §3 the basic low latitude momentum equation and an analytic flow field that will be an approximate solution. In §4 turbulent damping is evaluated, and §5 shows the resulting deposition rate of momentum into the flow from a representative pair of oppositely running g-modes. Results from the simple analytic solution are given in §6, and limitations of the model are discussed in §7.

2. FLOWS DEEP IN THE SUN DRIVEN BY g-MODES

To understand the proposed wave mechanism it is important to appreciate the dynamical conditions of the environment below the convective envelope in which the zonal flow is observed. Figure 1a shows the steady flow speeds in the tachocline from the analytic fits of Charbonneau, *et al.* (1999) to helioseismic measurements. This differential rotation will be ignored compared to the larger velocities V that we will consider for the 1.3 yr reversing flow. The flow is drawn as a wave travelling downward with diminishing amplitude. The approximate midpoint of the observed flow, $r_m = 0.675R_\odot$, is marked with a dotted line. It is well established that solar flows below the CE cannot cause turbulence in the vertical because the velocity shears are not large enough to overcome convective stability (Spiegel & Zahn 1992). But convective overshoot can cause a weak ambient turbulent diffusivity in the vertical direction (Fig. 1b, dashed lines) as well as radiative diffusivity. The turbulent diffusivity was derived by Montalban & Schatzman (2000) from convective overshoot in one and two dimensional models and stated in terms of ambient temperature, which we converted to radial distance using a standard solar model. By comparison, horizontal diffusivities D are much larger. The two dashed lines in Figure 1c roughly bound estimates by Schatzman (1996); Talon, Kumar, & Zahn (2002) of D due to gravity waves generated by plumes from the CE.

In our model, the dominant source of D is turbulence generated by the reversing flow itself (§4). The solid lines show this D for model flows whose maximum speed at r_m is either 5 or 50 m/s. This turbulence is a prerequisite for dissipating the g-modes so they can drive the flow. The turbulence develops because the zonal flow occurs mainly at low latitudes making its horizontal gradients sufficiently large to overcome an angular momentum hurdle and generate turbulence.

In the proposed mechanism, the g-modes carry net energy up from the solar core and encounter this turbulence, causing them to deposit some of their momentum flux into the zonal flow. As the flow develops it builds up the horizontal turbulence which is also diffusing energy away from the flow. With the resulting diffusivity being proportional to the magnitude of the flow, independent of direction, the system is inherently non-linear such that it produces a natural cap on the flow to determine its peak speed.

The other process important for the reversing flow is wave filtering. As the waves build up the flow in one or the other direction, they are selectively dissipated in that direction by the Doppler effect. The resulting imbalance in the wave momentum flux then favors the build up of the flow in the opposite direction higher up. While the flow dissipation discussed earlier is determined by flow speed, the wave filtering is most important where the vertical gradient of the speed is large.

Following Paper I, we shall present an analytic formulation of the proposed mechanism and apply it to the solenoidal (divergence free) zonal momentum budget at the equator. Since the Coriolis force vanishes at the equator, the compressible meridional winds do not come into the picture nor does the energy budget of its flow. Thus it is justified, to first approximation, that the momentum budget of the flow at the equator is treated in the framework of a one-dimensional model – the “prototype model” introduced by Lindzen & Holton (1968) for the terrestrial quasibiennial oscillation. In reality the problem is two dimensional. Away from the equator, the meridional circulation comes into play and redistributes the momentum such that the flow is naturally confined to low latitudes.

Restricting the analysis to the equatorial region, we postulate that (a) the flow oscillation propagates down having a wavelength consistent

with the observations and (b) the amplitude declines with depth. Since the proposed wave mechanism is inherently non-linear, only a simplified analytic solution of the zonal momentum equation is presented. The real and imaginary components yield estimates of the magnitude of the reversing flow in terms of g-mode properties: amplitude, angular harmonic, oscillation period.

3. MOMENTUM BALANCE

Relative to spherical coordinates r, θ, ϕ rotating with the nonconvecting solar interior, write the east-west flow velocity, $\phi V(r, t)f(\theta)$. Its divergence is zero. Conservation of the ϕ component of momentum

$$\rho \frac{\partial V}{\partial t} f = \hat{\phi} \cdot \nabla \cdot \Pi + \frac{\dot{J}}{r \sin \theta} \quad (1)$$

determines the flow near the equator; Π is the turbulent stress tensor that diffuses the flow's momentum, \dot{J} is the rate per unit volume at which angular momentum is deposited into the flow by g-modes, and the density ρ is taken independent of time. The right member is evaluated in §4 and §5 for the following model flow field.

As mentioned earlier, pure zonal flow is unrealistic sufficiently far from the equator. A latitudinal Coriolis force emerges to drive a weak meridional flow that reduces the zonal flow at higher latitudes. By latitude 30° , V is observed to be zero (Howe, *et al.* 2000). We model this by setting $f(\theta) = 1 - 4 \cos^2 \theta$ and consider only low latitudes, say $\theta \approx 90^\circ \pm 20^\circ$. The radial dependence is modelled as a wave of frequency ω and wavenumber k sinking into the Sun,

$$V(r, t) = A(r) e^{i[\omega t + k(r - r_m)]}, \quad (2)$$

where $r_m = 0.675 R_\odot$ is near the midpoint of the observed flow and the amplitude, $A = V_0 \exp[k_A(r - r_m)]$, declines with depth. We will use $V_0 = 50$ m/s in a numerical example. But other values are possible because the observations of Howe, *et al.* (2000) do not determine a unique value for V_0 or k . The limited radial resolving power of their measurement determines only a family of possible pairs (V_0, k) any of which would appear to give their reported peak speed of about 5 m/s. This family is plotted on Figure 2, assuming as in Paper I that their radial resolution has

a full width at half height of $0.075 R_\odot$. Setting $k_A = 10/R_\odot$ permits the approximation $k_A \ll k$. Then radial derivatives of A , ω and k can be ignored and $\partial V / \partial r = ikV$.

4. EFFECTS OF TURBULENCE

4.1. Two Dimensional Turbulence

The observed latitudinal shear is strong enough to be unstable. The resulting turbulent motion occurs on spherical surfaces because of extreme stability in the radial direction (Spiegel & Zahn 1992). A mathematical study by Watson (1981) showed that radially stable layers of a slowly rotating star are horizontally unstable when $B > 0.29$ in the differential rotation curve, $\Omega(\theta) = \Omega_0(1 - B \cos^2 \theta)$, often applied to solar data. Since our model flow has an effective B one order of magnitude larger, it should be strongly turbulent even though we do not consider polar regions as does the Watson (1981) study. Using $\Delta\theta = 30^\circ$, the turbulence has a latitudinal forcing scale $L \approx r_m \Delta\theta = 250$ Mm. Its characteristic time $\tau \sim L|V|^{-1} = 0.16$ yr for an equatorial flow velocity $V = 50$ m s⁻¹. The largest turbulent scales (L and $L/2$) carry off most of the flow's energy and momentum since energy in 2D turbulence falls steeply as the cube of the scale (Tabeling 2002; Paret, Jullien, & Tabeling 1999). Only about 10% of turbulent energy is in scales $L/3$ and smaller.

A proper estimate of turbulent diffusion needs to account for the flow's downward drift. Figure 3 shows $|V|$ at some instant and the arrow indicates how far this pattern will move in a time 2τ . (Turbulence stimulated by V at some instant becomes fully developed after a time τ and decays after a similar time interval.) Thus turbulence has to be computed from some weighted average of $|V|$ that prevailed during the recent past at a given location. It's clear from the figure that the effective velocity forcing the turbulence will be a wiggling curve with mean height close to $2A/\pi$. The wiggles will be ignored and the effective turbulent velocity $V_t \equiv 2A/\pi$. Then horizontal diffusivity caused by the flow is simply

$$D \sim LV_t \quad (3)$$

4.2. Damping of Flow

In equation (1) only two elements ($\Pi_{\theta,\phi}$ and $\Pi_{r,\phi}$) of the symmetrical stress tensor can contribute because of zonal symmetry. The latter element is zero since vertical eddy viscosity is negligible in this part of the Sun. The remaining element has the mathematical form in spherical coordinates,

$$\hat{\phi} \cdot \nabla \cdot \Pi = \frac{1}{(r \sin \theta)^2} \frac{\partial}{\partial \theta} \left[\rho D \sin^3 \theta \frac{\partial}{\partial \theta} \left(\frac{Vf}{\sin \theta} \right) \right] \quad (4)$$

where ρD is the horizontal eddy viscosity. Since f has the dominant θ dependence near the equator, equation (4) reduces to $\hat{\phi} \cdot \nabla \cdot \Pi = 8\rho D V r^{-2} \cos(2\theta)$. This term removes momentum from the flow and, being nonlinear in velocity amplitude ($DV \propto A^2$), it will limit the strength of the flow.

4.3. Damping of g-modes

Turbulence also removes energy from the g-modes but diffusion theory does not apply since the main turbulent scales are larger than g-mode horizontal scales of interest here. Instead, horizontal advection in random directions is the main physical loss mechanism, as suggested by the referee of Paper I. Recall that the kinetic energy of a linear oscillation is converted into potential energy twice each oscillatory cycle. For g-modes this consists of work done against buoyancy and it is temporarily stored as a local temperature fluctuation. Advection from turbulent eddies in the flow transports the thermal variation horizontally. That weakens its ability to drive the next velocity cycle of the g-mode because it is misaligned with the rest of the global oscillation. The $1/e$ decay time of local energy is approximately the time it takes the effective turbulent velocity to carry fluid a distance k_h^{-1} , where $k_h = \ell^*/r$ is the horizontal wavenumber of the g-mode and $\ell^* = \sqrt{[\ell(\ell+1)]}$. The inverse is the decay rate of local g-mode energy due to turbulent advection,

$$\kappa \sim k_h V_t. \quad (5)$$

5. MOMENTUM DEPOSITION BY g-MODES

Local dissipation of a g-mode causes it to deposit momentum flux in the same layers. The ba-

sic relation is derived for a single pair of g-modes as was done, e.g., by Kim & MacGregor (2003) and in Paper I. In future work, one could sum such results over all mode pairs thought to be active. Let U^\pm be the horizontally averaged kinetic energy density of a prograde(+) and retrograde(-) g-mode having identical radial and angular harmonic numbers (n, ℓ, m) except that the azimuthal numbers m have opposite signs. In the slowly rotating Sun, such mode pairs have the same oscillation frequency σ_0 except for negligible high order terms. Per unit volume of fluid, each mode deposits energy at the rate κU^\pm and angular momentum at the rate $(2m/\sigma^\pm)\kappa U^\pm$ (Zahn, Talon, & Matias 1997; Paper I 2004). This momentum concentrates at low latitudes since modes with $|m| \approx \ell$ are the most effective (§6.1). The Doppler-shifted oscillation frequency applies: $\sigma^\pm = \sigma_0(1 \mp \beta)$ where $\beta = V|c_\phi|^{-1}$ and $c_\phi = \sigma_0 m^{-1} r \sin \theta$ is the zonal phase velocity of the g-mode. Summing the effect of the two g-modes and using $\beta^2 \ll 1$, angular momentum is deposited into the fluid at a rate per unit volume,

$$j = \frac{2|m|}{\sigma_0} \kappa (U^+ + U^-)(\beta + \epsilon). \quad (6)$$

The β term steepens shear and $\epsilon \equiv (U^+ - U^-)(U^+ + U^-)^{-1}$ causes the flow to drift down toward the incident wave energy because of unequal cumulative damping of the two oppositely running waves.

Choose some deep reference level r_1 where the flow is negligible and assume the two g-modes have the same energy density there: $U^+(r_1) = U^-(r_1) \equiv U_1$. Above this level turbulent advection attenuates the energy density as

$$U^\pm(r > r_1) = U_1 e^{-\alpha^\pm}, \quad (7)$$

where $\alpha^\pm = \int_{r_1}^r dr \kappa v_g^{-1}$ (Zahn, Talon, & Matias 1997), $v_g = (\sigma^\pm)^2 (N k_h)^{-1}$ is the g-mode's upward group velocity. Vertical wavenumber k_v was eliminated from group velocity using the dispersion equation $(k_h/k_v)^2 = \sigma^2(N^2 - \sigma^2)^{-1}$ with $\sigma^2 \ll N^2$. Equation (7) defines α with respect to energy as is customary. (Paper I wrongly defined α to attenuate amplitude, making α half as large). Expanding the Doppler factor,

$$\alpha^\pm \approx \frac{1}{\sigma_0^2} \int_{r_1}^r dr \kappa k_h N (1 \pm 2\beta). \quad (8)$$

Name the two parts such that $\alpha^\pm \equiv \bar{\alpha} \pm \delta$ and insert into equation (7). It follows that $\epsilon = -\tanh(\delta)$ and, since $\delta^2 \ll 1$ for conditions studied in this paper, $\epsilon = -\delta$.

The main g-mode attenuation occurs through the exponent $\bar{\alpha}$, which is shown on Figure 4a for several values of V_0 and the case $\ell = 50$, $\sigma_0 = 1.1 \times 10^{-4} \text{ s}^{-1}$. To calculate other cases use $\bar{\alpha} \propto V_0 \ell(\ell+1) \sigma_0^{-2}$. The integrand for δ contains a rapidly varying factor $e^{ik(r-r_m)}$ permitting the slower radial dependences to be moved outside the integral sign. The result near the equator is

$$\epsilon = -\delta \approx \frac{i}{|c_\phi|} F_\epsilon V_t V. \quad (9)$$

where $F_\epsilon = 2Nk_h^2(k\sigma_0^2)^{-1}$. A factor, $V(r) - V(r_1)$, was approximated as $V(r)$ by choosing a lower limit $r_1 = 0.4R_\odot$ that is below the large flow velocities. Figure 4b shows the real parts of ϵ and β . Since the latter is proportional to V and therefore the flow's angular momentum, one can see that the ϵ term will add angular momentum (equation 6) with the proper sign and phase to move the entire flow downward.

6. RESULTS

6.1. Analytic Solution

Now the zonal momentum equation (1) can be reduced to algebraic form with equations (4 & 6) and the flow field in equation (2). The result near the equator, with $\sin\theta \approx 1$ is,

$$i\omega V + \frac{8L}{r^2} V_t V = F_1(V + iF_\epsilon V_t V) \quad (10)$$

where $F_1 \equiv 2m^2 \kappa(U^+ + U^-) \rho^{-1} (\sigma_0 r)^{-2}$. Recall that the effective turbulent velocity V_t is positive and proportional to the amplitude of V , showing that two terms are nonlinear in flow amplitude. After cancelling the common factor V , real and imaginary terms must balance separately. The real terms require $F_1 = 8LV_t r^{-2}$. Substituting this in the definition of F_1 gives a condition on how much g-mode energy density is needed to drive the flow,

$$U^+ + U^- = \frac{4L\rho}{k_h} \left(\frac{\sigma_0}{m} \right)^2. \quad (11)$$

It declines at least as fast as m^3 (precisely, as $\ell^* m^2$), which demonstrates how much more efficient are high zonal harmonics of a given ℓ for

driving the flow. The g-mode power dissipated per unit volume is $\kappa(U^+ + U^-)$ and declines as m^2 . Equating the imaginary terms and eliminating F_1 gives the forcing velocity for horizontal turbulence,

$$V_t = \frac{r\sigma_0}{4k_h} \left(\frac{\omega k}{LN} \right)^{\frac{1}{2}}, \quad (12)$$

that is needed for a self consistent flow solution. It is inversely proportional to ℓ^* because of the factor k_h .

Although radial derivatives of ω and k were ignored, our mathematical approximation still allows them to be weak functions of r . Equation (12) constrains the radial dependence of ωk to be proportional to $NV_t^2 r^{-4}$. But additional physics coupling layers vertically may be needed to fully determine the radial dependences of flow parameters A , ω and k . A numerical integration of the differential equations seems to be the next step needed and, if practical, it should include the weak transient meridional circulations that must accompany a reversing zonal flow.

6.2. Numerical Values

Many different arrays of g-modes could cause the observed flow velocity and 1.3 yr period. Here we display "typical" g-mode pairs (prograde and retrograde), each of which could drive the observed flow if that pair acted alone. Future workers could use this as a guide to choosing arrays of modes for computing their combined effect. The typical mode for driving the flow will be one in which $|m| \approx \ell$ because of the very high efficiency (§6.1) of modes with large $|m|$. We substitute $|m| = \ell = \ell^*$ in the formulas to simplify the next two figures. This is minor compared to the order of magnitude uncertainties faced earlier in evaluating turbulence. After finding sets of parameters needed to drive the flow on and near the sphere $r = r_m$, we briefly mention radial dependence.

At r_m there is only one free parameter V_0 describing the flow. Figure 2 assigns a compatible radial wavenumber and the frequency $\omega = 2\pi(1.3 \text{ yr})^{-1}$ is observed. Three parameters describe the typical g-mode pair; namely, ℓ , σ_0 and the energy density. Equations (11 & 12) constrict this four-fold freedom to two free parameters. Observers care more about the velocity amplitude u_{typ} of the typical g-mode so we replace energy density by

writing $(U^+ + U^-) = \frac{1}{2}\rho[(u^+)^2 + (u^-)^2] \equiv \rho u_{typ}^2$. Then equation (11) gives $u_{typ} = 2\sigma_0(Lr\ell^{-3})^{\frac{1}{2}}$. This velocity for one g-mode will be very large because it is intended to stand for the total effect of thousands of g-modes of similar scale. Figure 5a shows how much local mode velocity is needed when the typical mode has a given angular harmonic and oscillation frequency. Figure 5b shows a similar plot for the peak flow velocity at r_m , derived from Equation (12) and the relation on Figure 2. When observational resolution improves to the point that k and therefore V_0 are known, Figure 5b will provide a relation $\sigma_0 = f(\ell)$ indicating what range of radial harmonics are participating. This would reduce to one, the present two parameter (σ_0, ℓ) uncertainty about typical states of g-modes that drive the flow.

If the energy density of the typical state were equally distributed over N_m modes of comparable horizontal and vertical scale, then the amplitude of a single mode would be $u_m \approx u_{typ}N_m^{-0.5}$. For example, the case marked with plus signs on Figure 5 has $u_{typ} = 210$ m/s. If its energy is spread over 1000 modes, $u_m = 6.6$ m/s. Amplitudes are strongly reduced in the convective envelope by the factor $q = (r_b/r_t)^\ell(\rho_b/\rho_t)^{0.5}$ where b identifies the bottom of the convection and t the top location where radiative and convective losses can reasonably be ignored. The dashed curves in Figure 5a show where $qu_m = 1$ mm/s at $r_t = 0.99R_\odot$ for the cases of 100 and 10000 modes. Oscillation amplitudes are < 1 mm/s to the right of the appropriate dashed curve. Thus most of the g-mode states covered by the figure would be unobservable at the solar surface by their oscillatory motion.

For a given array of active g-modes, an east-west flow field centered deeper in the Sun would almost certainly have an oscillation period different from 1.3 yr. That is because equation (12) solved for ω would have five radially dependent factors in its right member. In other words, each depth has a "natural period". But physically the period has to be the same over the shell containing the flow, otherwise wave filtering by lower layers would fall out of phase with the flow above and fail to reverse the upper part of the flow properly. The top part of the flow would become more chaotic than periodic. We suggest that this is what limits the thickness of the shell containing the flow. The nat-

ural periods within the shell must be sufficiently similar so that they can lock together and act with one period. Solar observations show that the shell over which this has occurred is about $0.1R_\odot$ thick.

7. DISCUSSION AND SUMMARY

There are some obvious limitations to this simple model. It considers only two dimensional motions in the equatorial region. More complex three dimensional flows at higher latitudes are likely to feed back and modulate the diffusivity at the equator, affecting the flow predicted by our model. Also, we forced the vertical profile of flow velocity to be a radially damped sine wave. During the time this flow wave drifts down by a wavelength divided by 2π , neither the radial shear of the flow nor its downward speed is allowed to vary by much. But in reality, each should fluctuate about its mean trend because each is partially controlled by a sinusoidal function; respectively, β or ϵ on Figure 4. Numerical integrations of the equations of motion are more appropriate to investigate such details. But analytic or numerical, the large uncertainties in estimating turbulence will underlie all results.

If g-modes are indeed driving the zonal flow observed above $0.6R_\odot$, then they should also drive flows in the rest of the Sun's nonconvecting interior. Their reversal periods $2\pi/\omega$ would probably be different from 1.3 yr. Discovery of a new zonal flow in deeper layers would lend important support to the overall approach in this paper. The model applies to any depth in the nonconvecting interior but, being designed for a thin shell, should be applied to only one flow system at a time. If a deeper flow has a longer reversal period, it might be detected first by the way its wave filtering imposes a time dependent bias on the mean velocity of the currently observed 1.3 yr flow.

In summary, the horizontal turbulence of the flow itself causes a larger diffusivity than any used previously to study these solar flows (Figure 1). The larger D was very helpful in matching the observed 1.3 yr period without appealing to g-modes of extremely large angular harmonic ℓ or very low oscillation frequency σ_0 . We found two analytic relations (eqs. [11 & 12]), between a reversing zonal flow and its driver—a pair of oppositely running g-modes. The pair is supposed to typify those

high harmonics that are primarily responsible for driving the flow. For a wide range of g-mode parameters (ℓ, σ_0), Figure 5 shows compatible values for peak flow velocity V_0 and g-mode amplitude u_{typ} . In most of the cases, g-mode amplitudes at the solar surface would be unobservably weak (§6.2).

The observations still permit a large range of flow velocities and radial wavenumbers (Fig. 2). Our use of $V_0 = 50$ m/s in examples does not exclude the possibility that its real value might be smaller or larger. Finally, there is another branch of solutions to equation (1) in which $\beta^2 \ll 1$ is not true. This would be needed if r-modes, not g-modes, turn out to be the main drivers of the 1.3 yr flow system.

REFERENCES

- Antia, H. M. & Basu, S. 2000, *ApJ*, 541, 442
- Basu, S., Christensen-Dalsgaard, J., Schou, J., Thompson, M. J., & Tomczyk, S. 1996, *Bull. Astron. Soc. India*, 24, 147
- Basu, S., et al. 1997, *MNRAS*, 292, 243
- Basu, S., et al., 2000, *ApJ*, 535, 1078
- Bretherton, F. P. 1969, *Quart. J. Roy. Meteorological Soc.*, 95, 213
- Brun, A. S., Turck-Chieze, S., & Zahn, J. P. 1999, *ApJ*, 525, 1032
- Charbonneau, P., et al. 1999, *ApJ*, 527, 445
- Christensen-Dalsgaard, J. & Berthomieu, G. 1991 in *Solar Interior & Atmosphere*, eds. A. N. Cox, W. C. Livingston, & M. S. Mathews (U. Arizona Press, Tucson)
- Cowling, T. G. 1941, *MNRAS*, 101, 367
- Dunkerton, T. J. 1997, *J. Geophys. Res.*, 102, 26053
- Elliott, J. R. & Gough, D. O. 1999, *ApJ*, 516, 475
- Fritts, D. C., Vadas, S. L., & Andreassen, O. 1998, *A&A*, 33, 343
- Guenther, D. B., Demarque, P., Kim, Y.-C., & Pinsonneault, M. H. 1992, *ApJ*, 387, 372
- Hines, C. O. & Reddy, C. A. 1967, *J. Geophys. Res.*, 72, 1015
- Howe, R., et al. 2000, *Science*, 287, 2456
- Kim, E.-J., & MacGregor, K. B., 2001, *ApJ*, 556, L117
- Kim, E.-J., & MacGregor, K. B., 2003, *ApJ*, 588, 645
- Komm, R., Howe, R., Durney, B. R., & Hill, F. 2003, *ApJ*, 586, 650
- Kosovichev, A. G., et al. 1997, *Sol. Phys.*, 170, 43
- Lindzen, R. S. & Holton, J. R. 1968, *J. Atmospheric Sci.*, 25, 1095
- Mayr, H. G., Mengel, J. G., Reddy, C. A., Chan, K. L., & Porter, H. S., 1997, *J. Geophys. Res.*, 102, 26093
- Mayr, H. G., Mengel, J. G., Reddy, C. A., Chan, K. L., & Porter, H. S., 2000, *J. Atmos. Sol.-Terr. Phys.*, 62, 1135
- Montalban, J. & Schatzman, E. 2000, *A&A*, 354, 943
- Paret, J., Jullien, M.-C., Tabeling, P. 1999, *Phys. Rev. Lett.*, 83, 3418
- Plumb, R. A. 1977, *J. Atmos. Sci.*, 34, 1847
- Ringot, O. 1998, *A&A*, 335, L89
- Schatzman, E. 1993, *A&A*, 279, 431
- Schatzman, E. 1996, *J. Fluid Mech.*, 322, 355
- Schatzman, E., Zahn, J.-P., & Morel, P. 2000, *A&A*, 364, 876
- Spiegel, E. A. & Zahn, J.-P. 1992, *A&A*, 265, 106
- Talon, S. & Charbonnel, C. 2003, *A&A*, 405, 1025
- Talon, S., Kumar, P., & Zahn, J.-P., 2002, *ApJ*, 574, L175
- Tabeling, P. 2002, *Phys. Reports*, 362, 1
- Watson, M. 1981, *Geophys. Astrophys. Fluid Dyn.*, 16, 285
- Wolff, C. L. 1983, *ApJ*, 264, 667

Wolff, C. L. 2002, ApJ, 580, L181

Wolff, C. L. & Mayr, H. G. 2004, ApJ, 606, L163,
(Paper I)

Zahn, J.-P. 1992, A&A, 265, 115

Zahn, J.-P., Talon, S., & Matias, J. 1997, A&A,
322, 320

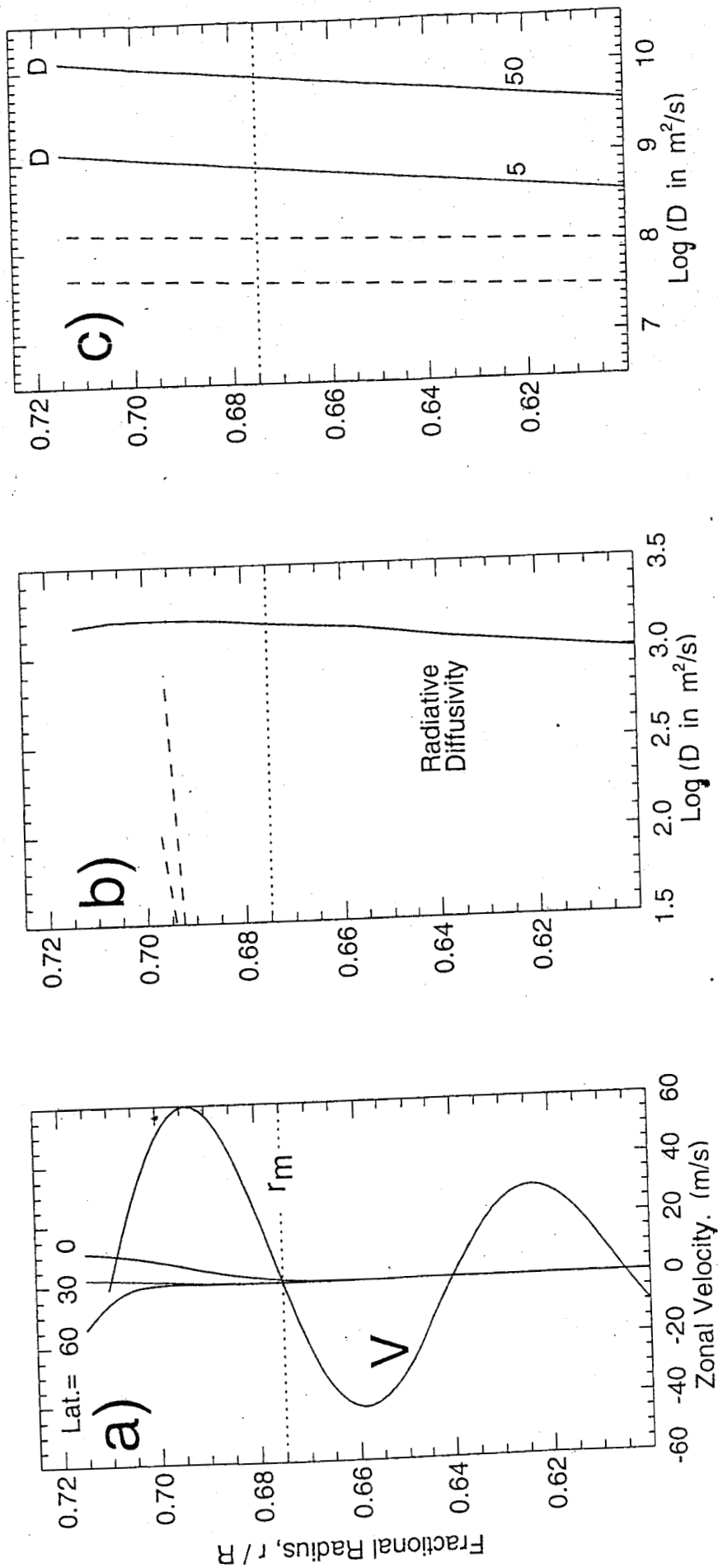


Fig. 1.— a) The observed relative speed of differential rotation at latitudes 0, 30 and 60 degrees is small compared to the 1.3 yr reversing flow, $V(\tau, t)$, as modeled in this paper. b) Radiative diffusivity and vertical turbulent diffusivity (dashed) are $< 1600 \text{ m}^2/\text{s}$. Each is negligible compared to (c), the horizontal diffusivity D caused by model 1.3 yr flows for which $V_0 = 5$ or 50 m/s . Convective overshoot creates a smaller horizontal diffusivity, estimated to lie between the dashed lines.

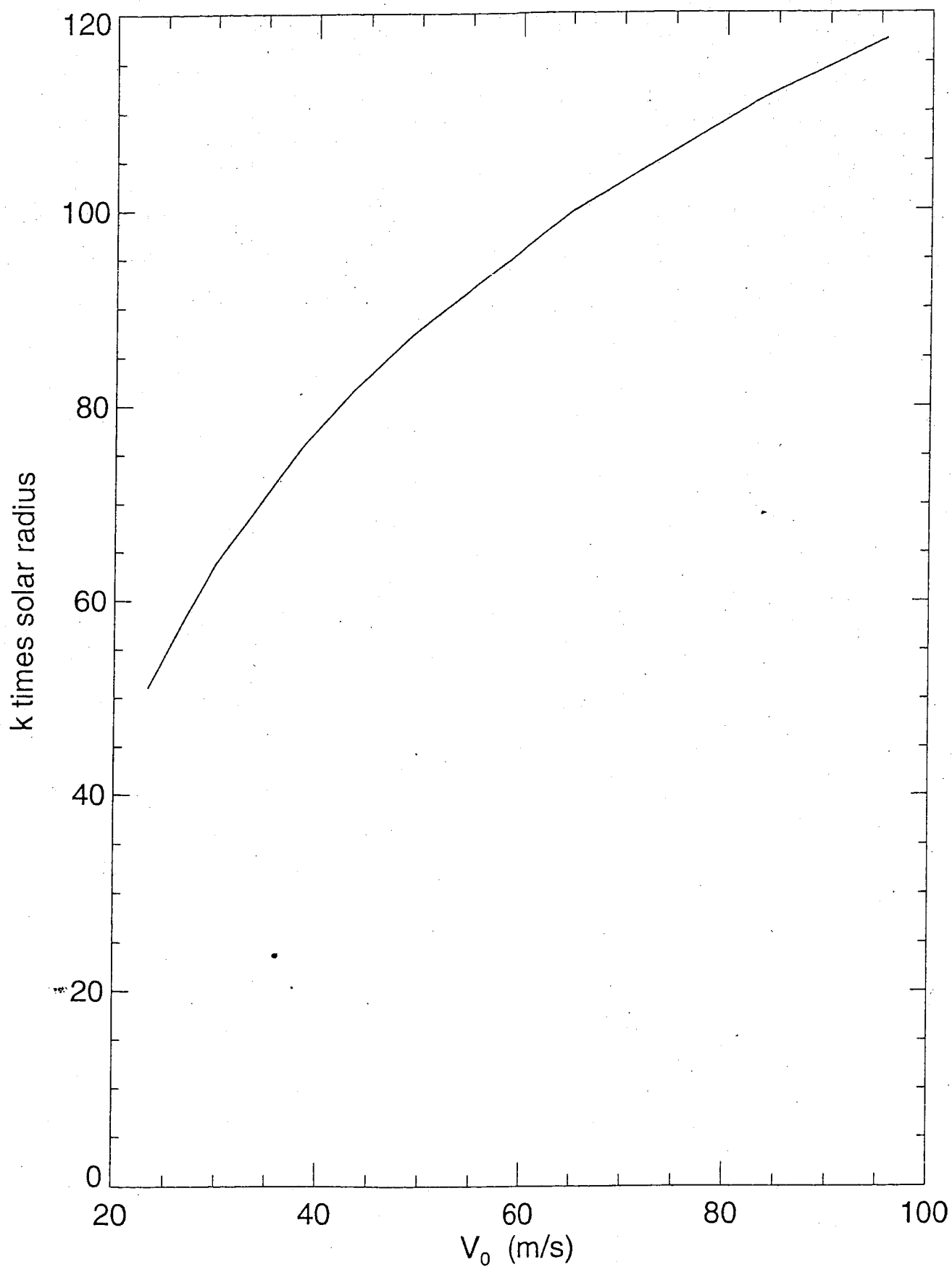


Fig. 2.— Zonal flow amplitude V_0 and radial wavenumber k that are mutually consistent with the observations of Howe, *et al.* (2000) near the radial midpoint of the flow. Future improvements in radial resolving power will restrict the range of possible V_0 and k values.

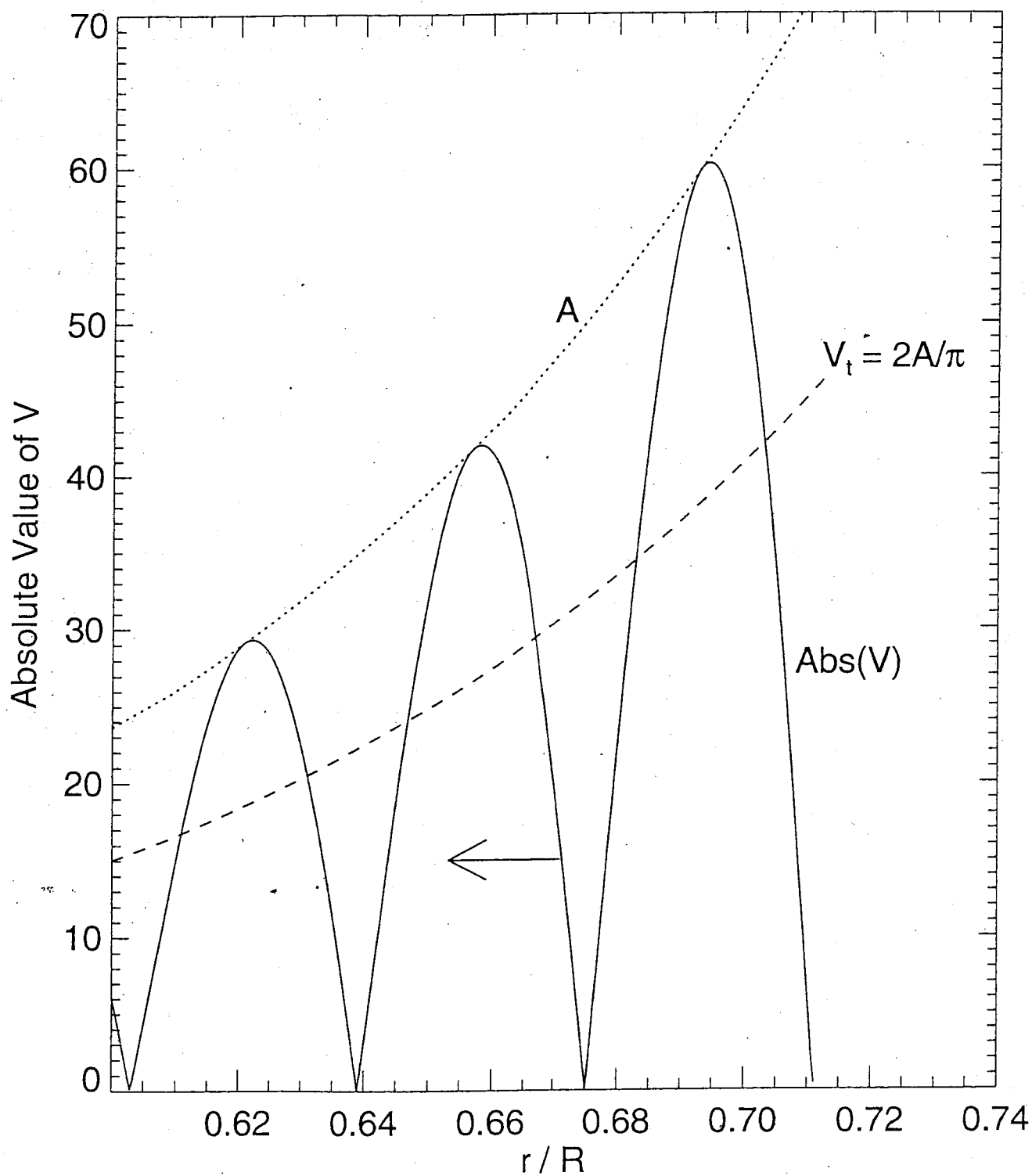


Fig. 3.— At any radial distance, the speed instantaneously driving turbulence, $|V|$, has a time averaged value of about $2A/\pi$ as this velocity field drifts downward within its envelope A . The arrow shows how far the field travels in a time 2τ . The dashed curve is used to define the effective velocity V_t forcing turbulence.

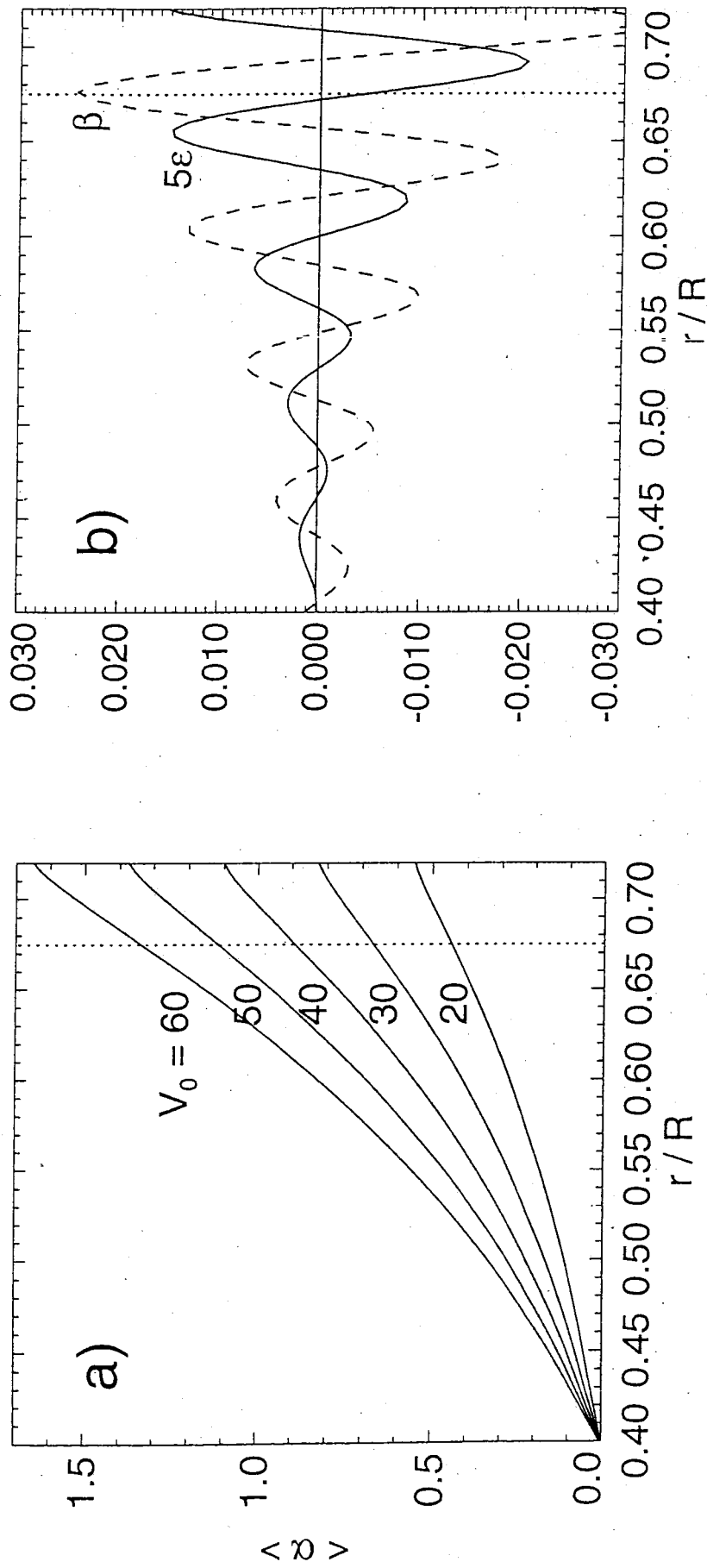


Fig. 4.— a) The mean attenuation exponent $\bar{\alpha}$ for g-modes encountering a model flow whose peak amplitude is V_0 at $r = r_m$. By assumption, attenuation begins at $0.4R_\odot$ where the flow is negligibly small. b) The real parts of the dimensionless factors affecting flow angular momentum in equation (6). For clarity ϵ is multiplied by 5.

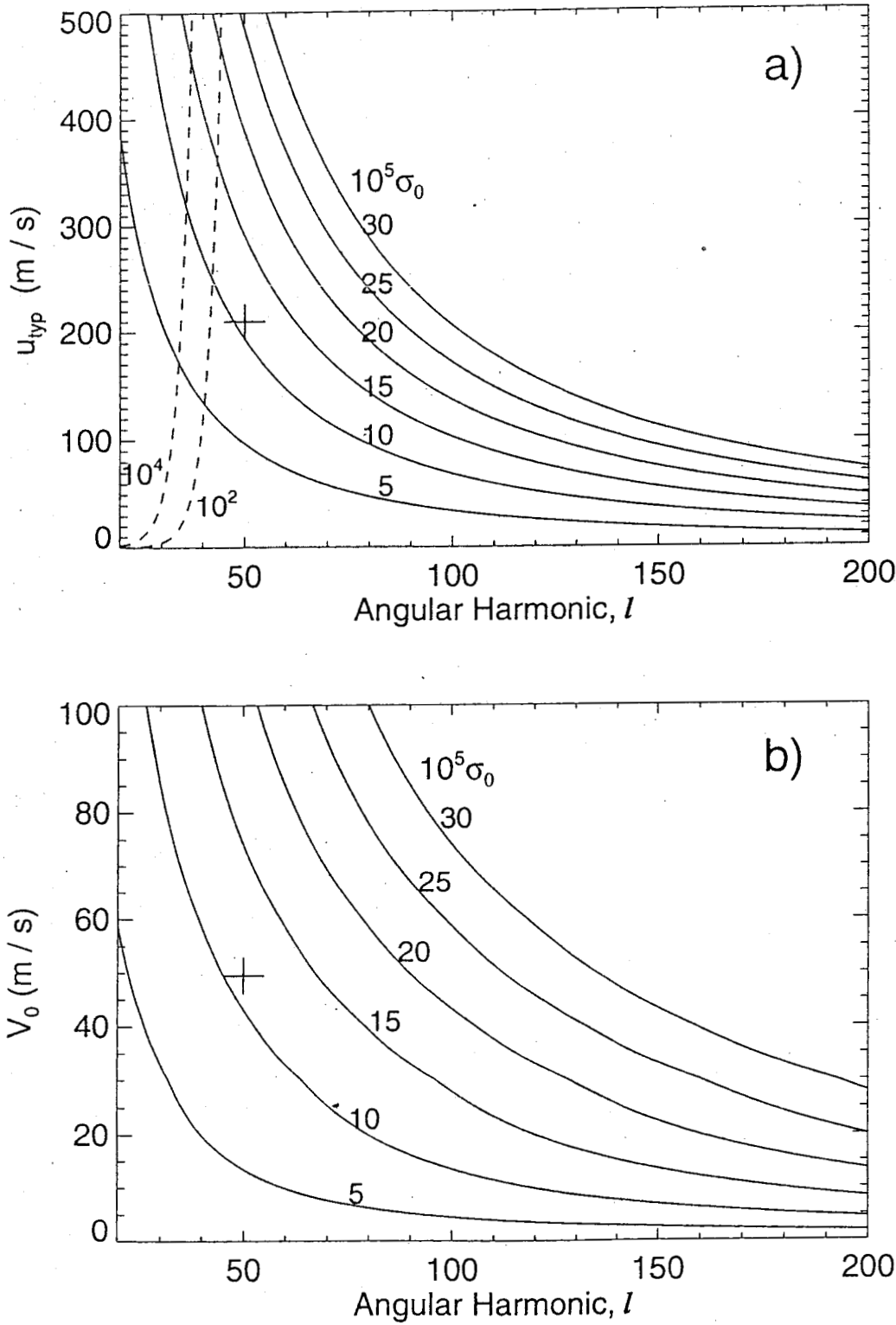


Fig. 5.— a) The g-mode amplitude u_{typ} and b) flow velocity amplitude V_0 required at r_m if the flow is entirely driven by one g-mode pair ($+m$ and $-m$) in the angular harmonic state ℓ with oscillation frequency σ_0 . If a pair with typical velocity u_{typ} had its energy distributed among 10^2 or 10^4 pairs of similar modes, each would have an amplitude < 1 mm/s at $0.99R_\odot$ for cases to the right of the applicable dashed curve. The plus sign marks a sample case discussed in the text. When new observations can severely constrain the possible values of V_0 , this figure will greatly reduce the combinations of ℓ and σ_0 that could reasonably be significant drivers of the flow.